Photodiagnosis and Photodynamic Therapy 26 (2019) 413–419

Contents lists available at ScienceDirect

Photodiagnosis and Photodynamic Therapy

journal homepage: www.elsevier.com/locate/pdpdt

Quantitative assessment of skin swelling using optical coherence tomography

Weijun Li[a], Peng Li[b], Yuhong Fang[a,c], Tim C. Lei[d], Kui Dong[a], Jian Zou[a], Wei Gong[a], Shusen Xie[a], Zheng Huang[a,d,*]

[a] Fujian Normal University, Key Laboratory of OptoElectronic Science and Technology for Medicine of Minister of Education, Fujian Provincial Key Laboratory of Photonics Technology, Fuzhou, China
[b] Shenzhen Certainn Technology Co., Ltd., Shenzhen, China
[c] Minnan Normal University, College of Physics and Information Engineering, Zhanghou, China
[d] University of Colorado Denver, Department of Electronical Engineering, CO, USA

ARTICLE INFO

Keywords:
Tissue swelling
Exfoliation
Histamine
OCT
Imaging

ABSTRACT

Background: Preclinical and clinical studies suggest that optical coherence tomography (OCT) is a useful tool to visualize inflammatory conditions.
Objective: The objective of this study was to evaluate the usefulness of combining OCT and various image processing techniques for quantitative assessment of histamine-induced tissue swelling.
Methods: Both time-domain and frequency-domain OCT were used on a mouse ear model. The ear thickness and volume before and after histamine challenge were determined from pixel locations in 2D scans and voxel number counting in 3D scans. Swelling kinetics was analyzed on 3D contour mapping. Microvessel network was visualized using speckle decorrelation analysis.
Results: OCT images showed that the thickness and volume changes were histamine dose and contact time dependent. The 3D mapping showed that the histamine-induced swelling spread slowly and directionally. OCT data indicated that microvessel opening and vessel dilation occurred prior to tissue swelling.
Conclusion: OCT is a robust and quantitative non-invasive imaging tool for assessing skin swelling.

1. Introduction

Cutaneous tissue swelling is one of important signs of inflammatory response [1]. Its quantification study is important but challenging. In rodent models, such response can be estimated by measuring the tissue thickness change of extremities including ears, paws and tails [2]. In particular, the mouse ear swelling test (MEST) developed in the early 1980s that involves the measurement of mouse ear thickness using a thickness gauge or a hand-held dial micrometer [3,4]. The histological examination and weight measurement of punch biopsy (ear disk) are also used in animal models for precisely assessing the severity of tissue swelling [5,6]. However, these conventional methods cannot meet the need for the precise non-invasive quantification of tissue swelling process.

Optical imaging modalities have the potential to provide quantitative morphological assessment of biological tissue non-invasively. Recently, optical coherence tomography (OCT) has been used as a virtual optical biopsy tool that enables tissue imaging at a micrometer resolution [7–9]. Two-dimensional (2D) and three-dimensional (3D) OCT imaging of the skin tissue can be used to visualize dermal edema, measure epidermal thickness and assess vascular networks [10–12]. OCT has also been used to exam photodynamic therapy (PDT)-induced skin morphological changes [13,14].

Histamine is a mediator of allergic inflammation released mainly from mast cells and strongly increases vascular permeability which is responsible for tissue swelling. Quantification of the ear thickness from ear punch biopsy has often being used in assessing histamine-induced vascular hyperpermeability [15,16]. An early study suggested that light attenuation coefficient changes of human skin induced by the intracutaneous administration of histamine can be detected by OCT [17].

This study utilized OCT to quantitatively evaluate micro-morphological changes in tissue swelling process. Imaging analysis techniques were applied to assess acetone-induced exfoliating and histamine-induced vascular responses in a mouse ear model. Results suggested that OCT is a robust non-invasive imaging tool for quantitative assessment of exfoliation and skin swelling.

* Corresponding author at: College of Photonic and Electronic Engineering, Fujian Normal University, Fuzhou 350007, China.
E-mail address: zheng_huang@msn.com (Z. Huang).

https://doi.org/10.1016/j.pdpdt.2019.04.030
Received 23 October 2018; Received in revised form 29 April 2019; Accepted 29 April 2019
Available online 01 May 2019
1572-1000/

2. Materials and methods

2.1. Time-domain OCT

This system (Shenzhen Certainn Technology Co., Ltd., Shenzhen China) used a light source (IPSDS0803, INPHENIX, Livermore CA, USA) with the center wavelength of 820 nm and 3 dB bandwidth of 40 nm. The output power of the light source was approximately 5 mW. Its reference arm utilized a rapid scanning optical delay line (RSOD) and the optical beam was modulated at 42 kHz.

2.2. Frequency-domain OCT

This system (Shenzhen Certainn Technology Co., Ltd.) was a sweep source OCT (SS-OCT) system and its light source (SSOCT1310, Axsun Technologies) had a center wavelength of 1310 nm with a 90 nm bandwidth. The diameter of the objective lens (GCL-010630, Daheng Beijing, China) in the scanning probe was 30 mm and its focal length was 50 mm. The A-scan speed of the system was 50k scans/s and the B-scan speed was 300 scans/s.

2.3. Preparing mice

SPF grade ICR mice (8 weeks old, 22 ± 2 g, n = 12) were obtained from Fuzhou Wu Experimental Animal Center. The white hair mice were kept under regular diet and lighting. The hairs on the dorsal side of the right ear were removed using depilatory cream prior to the experiment. Extra care was taken in this step in order to avoid possible injury to the ear skin. Under general anesthesia the mouse was secured on the scanning platform and the ear was typed to a glass cover slide to remain flat during OCT scans. The area with visually distinct pattern of vessel network was selected and marked for OCT scans.

2.4. OCT scans before and after acetone treatment

B-scan OCT images of a small area of the ear (640 × 400 pixels) was obtain using the time-domain OCT, followed by applying a drop of acetone solution (80%) to the dorsal surface of the scanned area. The residual acetone was carefully removed after 10 min. The same area was scanned again. Imaging analysis was performed to access the presence of the corneum layer before and after acetone pre-treatment.

2.5. OCT scans before and after histamine challenge

Histamine solutions (0, 40, 80, 160 mg/ml) were prepared by dissolving histamine (REGAL Biological Technology Development Co, Shanghai, China) in 80% acetone. A drop of histamine solution was applied to the dorsal surface of the right ear for up to 90 min and OCT images (1500 × 450 pixels) were obtained under the line scan mode at various time points before and after the application of histamine using the frequency-domain OCT. The changes of full-thickness of the mouse ear before and after histamine treatment were evaluated by the 2D cross-section images obtained from the line scans.

For imaging the changes of vessel network, histamine-treated area was scanned after high concentration histamine (160 mg/ml) was administrated for 20 min. Y scanning mode was then used to obtain 3D images of an area of 4.5 mm × 3 mm × 3 mm. In this process, a total of 1200 B-scan images on each of 300 positions were captured (i.e. four repetitive B-scans at each location).

2.6. OCT image processing

To determine the changes of skin thickness the middle section (320 × 400 pixels for time-domain OCT and 750 × 450 pixels for frequency-domain OCT) of the intensity image was converted to grayscale color map and followed by Gaussian blurring using a custom Python programing and the OpenCV library software (Open Source Computer Vision Library, version 3.4.2). The average gray value of each row was calculated and normalized to generate a gray value versus depth distribution curve. The difference value (DV) between two pixel locations of the dorsal surface and ventral surface was then used as the full thickness of the ear.

To evaluate the time course of the overall tissue volume change, a total of 300 consecutive B-scans, i.e. one each from four scans at each location, were selected for the 300 consecutive locations in the Y direction for each time point. The OCT raw data (300 × 300 × 600 pixels) before and after histamine challenge were then processed to render 3D volumetric images using the Avizo software. The edema volume was then determined by counting the voxel numbers [10].

To further explore the homogeneity of histamine-induced edema, the consecutive B-scans were selected for 300 consecutive locations in the X direction for each time point. The OCT raw data (300 × 300 × 600 pixels in the Z direction) before and after histamine challenge were then processed to generate 3D contour maps using Python programming.

To visualize blood vessels 3D OCT raw data were processed with amplitude decorrelation algorithm with high pass filtering to produce an overlaid blood vessel network in the frame size of 300 × 300 pixels [18]. The frame scale of the blood vessel network reproduced in the en face image was 3 mm × 3 mm. To further quantify vasculature changes, the vessel component ratio was calculated using the binary image mask method [19]. The relative ratio of white pixels per frame (i.e. representing blood perfusion) was calculated from overlay/en face images (Fig. 1).

2.7. Mechanic measurement of ear thickness

After OCT scan the thickness of the treated ears was also measured using a digital thickness gauge (Mini digital, EXPLOIT TOOLS Co., China). Its measurement range was 0–12.7 mm and accuracy was 0.01 mm. The average value of the ear thickness was calculated from three measurements.

3. Results

3.1. Visualizing acetone induced exfoliating

The cross section images showed that the changes of gray value corresponded well with the layered structure of the mouse ear. The intact thin stratum corneum was identifiable, i.e. a bright line at the outmost surface layer (Fig. 2a).

In the absence of acetone, there was no visible change in OCT image

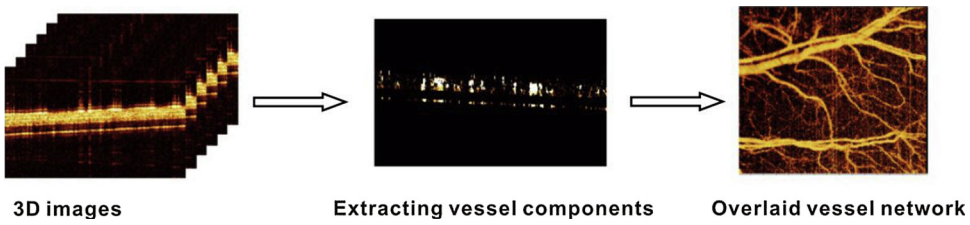

Fig. 1. Imaging processing steps for visualizing microvascular network.

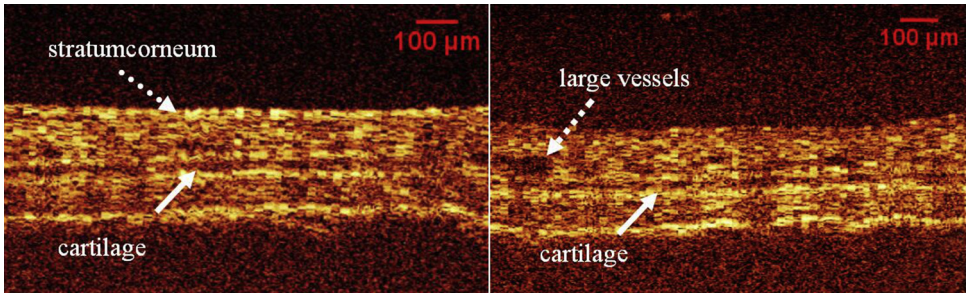

Fig. 2. Representative OCT images of mouse ear.
(A) Normal mouse ear and (B) after acetone-mediated exfoliating. Bar = 100 μm.

after applying the histamine aqueous solution of 160 mg/ml for up to 90 min. This suggested that histamine did not penetrate though the intact stratum corneum. After pre-treating the ear skin with acetone (80%) for 10 min the bright corneum line completely disappeared from the OCT image (Fig. 2b).

To quantify the exfoliation process, original OCT image was converted to a color map and a normalized grayscale distribution curve (i.e. grayscale versus pixel depth) was generated in terms of DV. The DV measurement indicated that the average full thicknesses of the scanned area before and after exfoliation were 330 ± 5 μm and 306 ± 5 μm (n = 3), respectively. Acetone induced a 7% reduction of the full skin thickness and this change was also visible in the DV curve as the corneum peaks disappeared (Fig. 3), which corresponded to the thickness of the stratum corneum layer of 24 ± 5 μm.

3.2. Quantifying histamine induced thickening

As shown in Fig. 4 the (top) dorsal layer and the (bottom) ventral layer could be precisely identified. The corresponding pixel depth locations were marked as the starting and ending points. The difference between the two end-points was used to determine the DV and the thickness of the mouse ear was derived from the DVs.

Fig. 5A shows the effect of the histamine dose and the treatment time on the skin thickness. At the A-scan position, the thicknesses of the mouse ear were estimated ranging from 60 to 85 DV, which were corresponded to 480 ± 20 μm to 680 ± 20 μm (n = 3). The initial decrease over the first 10 min observed in all three dose groups was likely caused by the removal of corneum layer by acetone. In average, at the dose levels of 40 mg/ml and 80 mg/ml, the overall thicknesses increased by 2.32% and 10.57%, respectively, over the course of 90 min. Whereas at the dose level of 160 mg/ml, the overall thickness increased by 38.48% over the course of 90 min. However, unlike the linear increase trend seen in 40 mg/ml and 80 mg/ml groups, when the dose level was increased to 160 mg/ml, the thickness quickly increased by 32.27% from 30 min to 50 min before reaching a plateau at 60 min.

Considering the variation of initial thickness of individual ears, the normalized ratios of thickness changes (i.e. net change) for each dose group were calculated using the time point of 10 min as the starting point so to exclude the effect of exfoliation on the thickness. As shown in Fig. 5B, net changes in thickness were more dramatic at the dose level of 160 mg/ml.

The comparison of OCT measurement and thickness gauge measurement showed that there were larger differences between two methods. The manual measurement by the gauge tended to overestimate the thickness by 1–3 folds (Table 1).

3.3. Quantifying histamine induced volume change

To determine the edema volume the 3D raw data were reconstructed from 300 B-scans of 300 locations (Fig. 6A). For an imaging field of view of 3 mm × 3 mm consisted of 300 B-frame locations with each location composed of 300 A-scans, the total number of pixel for the scanned volume of 300 × 300 × 600 pixels in the Z direction was 5.4×10^7 pixels, corresponding to a total voxel size of 4.5×10^{10} μm^3 (i.e. 3 mm × 3 mm × 5 mm). Based on the ratio of the scanned ear volume and the scanned total volume, the edema volumes of scanned area were calculated. Consistent with the changes of thickness, the volume increase at the concentration of 160 mg/ml was also more dramatic (Fig. 6B). The 3D image showed that edema mainly developed in the dermis layer above the cartilage on the histamine applied side.

3.4. Homogeneity in edema induced by histamine

Based on the 3D data reconstructed from the same FOV at different

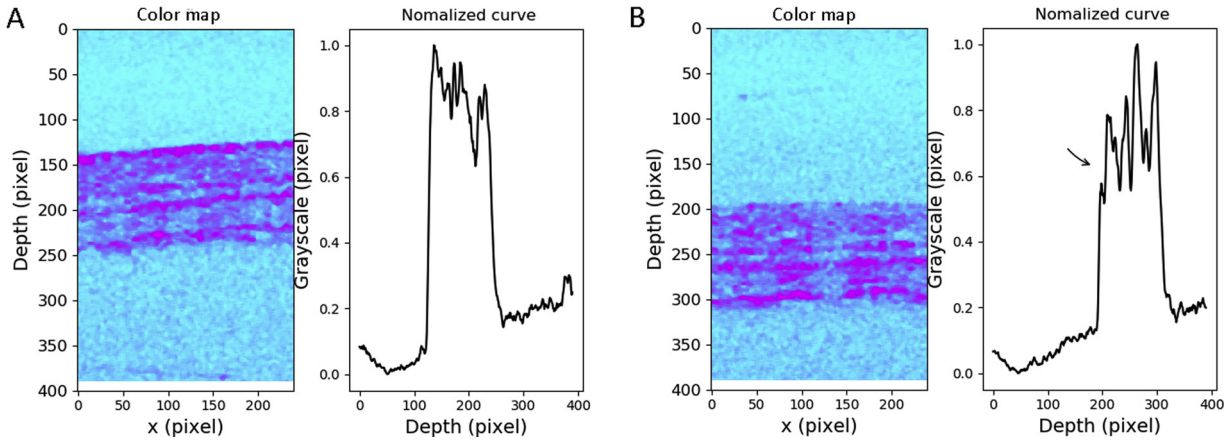

Fig. 3. Color map and normalized curve of gray value in longitudinal distribution.
(A) Before acetone treatment and (B) after acetone treatment. The black arrow indicates the disappearance of the corneum peaks.

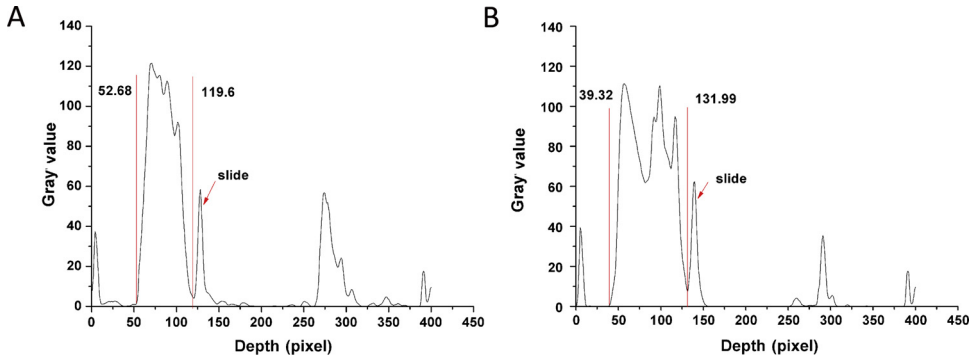

Fig. 4. The gray value longitudinal distribution.
(A) Before histamine treatment and (B) after 90 min of histamine treatment.

time points after histamine treatment (160 mg/ml), the net height of each pixels were obtained by subtracting the baseline (i.e. 0 min) and converted to 3D contour maps. The contour profile in the histamine treated region showed that the edema started from one corner and subsequently and slowly spread to the entire FOV. The homogeneity in the edema region seemed high (Fig. 7).

3.5. Quantifying vascular effect

Interestingly, although the thickness of the ear did not increase at the dose level of 160 mg/ml at the 20 min time point, the speckle decorrelation analysis showed significant changes of the vascular network (Fig. 8). To quantify the overall vascular change caused by histamine, vascular component ratios of the scanned area were calculated using binary image mask. Imaging analysis showed the blood perfusion increased from 13.6% to 24.5% (i.e. 10.9% increase).

4. Discussion

Preclinical and clinical studies suggest that dermal OCT is a useful tool to visualize some cancerous and inflammatory conditions [20,21]. Most OCT systems operate at 700 nm to 1300 nm, where light absorption and scattering by tissue components in the skin such as water, hemoglobin and melanin are relatively low [22]. The penetration depth of OCT is generally limited by multiple scattering and attenuation of the signal in the skin tissue. For skin diagnostics, the detection depth of 1 mm and the axial resolution of 15 μm are generally sufficient to differentiate the stratum corneum, living epidermis and upper parts of the dermis.

Table 1
Comparison of thickness changes measured by OCT and gauge at 90 min after histamine administration (mean ± S.D.).

Concentration (mg/ml)	OCT	Thickness Gauge
40 (n = 3)	2.32 ± 2.39 %	6.85 ± 6.38%
80 (n = 3)	10.57 ± 1.62%	28.01 ± 5.36%
160 (n = 3)	38.48 ± 1.61%	46.50 ± 6.47%

In addition to the visualization of micro-morphological structures, OCT can also be used to measure tissue optical properties including the scattering coefficient, the refractive index of living skin [20]. Welzel et al. showed that OCT was useful for detecting the small change in the light attenuation coefficient in the upper dermis caused by an increase of dermal water content induced by histamine [17]. For the intact skin, acetone is often used to facilitate the penetration of histamine.

The intensity analysis of OCT images has been used to identify the dermo-epidermal junction [17–23]. Similar approaches were used in this study to demarcate the stratum corneum layer. Initially, a time-domain OCT of 820 nm was used. The stratum corneum layer and exfoliating process were clearly visible on OCT images (see Fig. 2). To precisely determine the thickness of the stratum corneum layer the grayscale distribution curve was generated (see Fig. 3). The thickness of the stratum corneum in the dorsal side of adult white mouse ear was determined as 24 ± 5 μm (n = 3).

To investigate tissue swelling a frequency-domain OCT of 1300 nm was used. The full thickness of the ear was derived from the grayscale distribution curve before and after histamine treatment (see Fig. 4). At the dose levels of 40 mg/ml and 80 mg/ml, the overall thicknesses

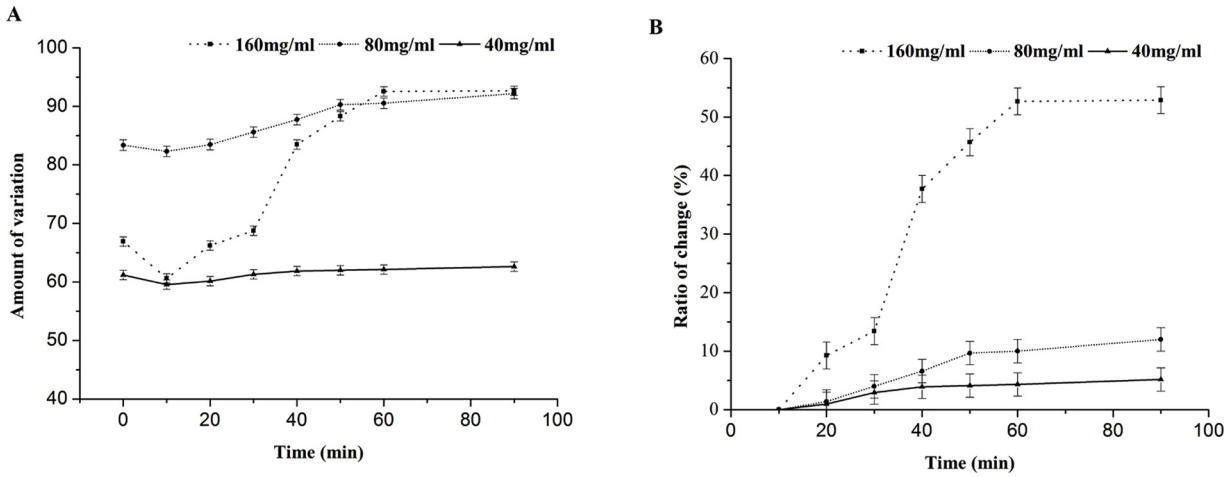

Fig. 5. Effect of histamine on ear thickness.
(A) Ear thickness derived from DV at different time points. (B) Ratio of changes in thickness over time.

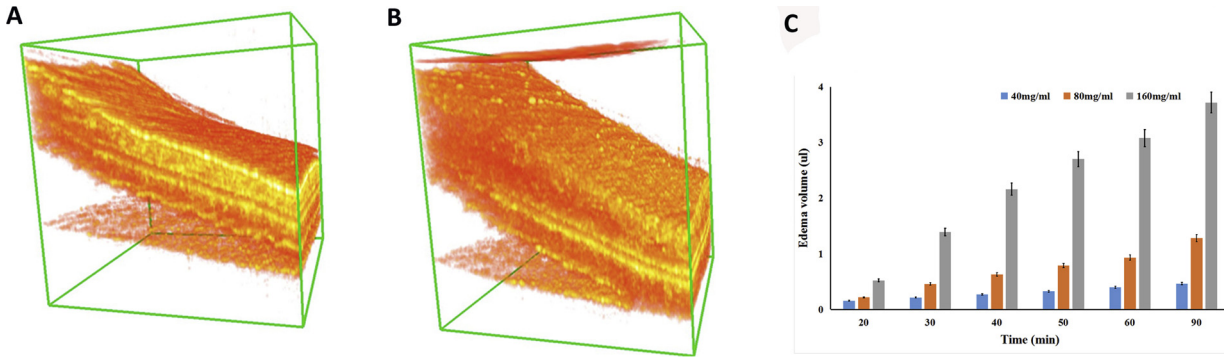

Fig. 6. Volume assessment.
(A) 3D images of reconstructed volumes before histamine treatment and (B) 90 min after histamine (160 mg/ml) treatment. (C) Time course of the volume change after histamine treatment.

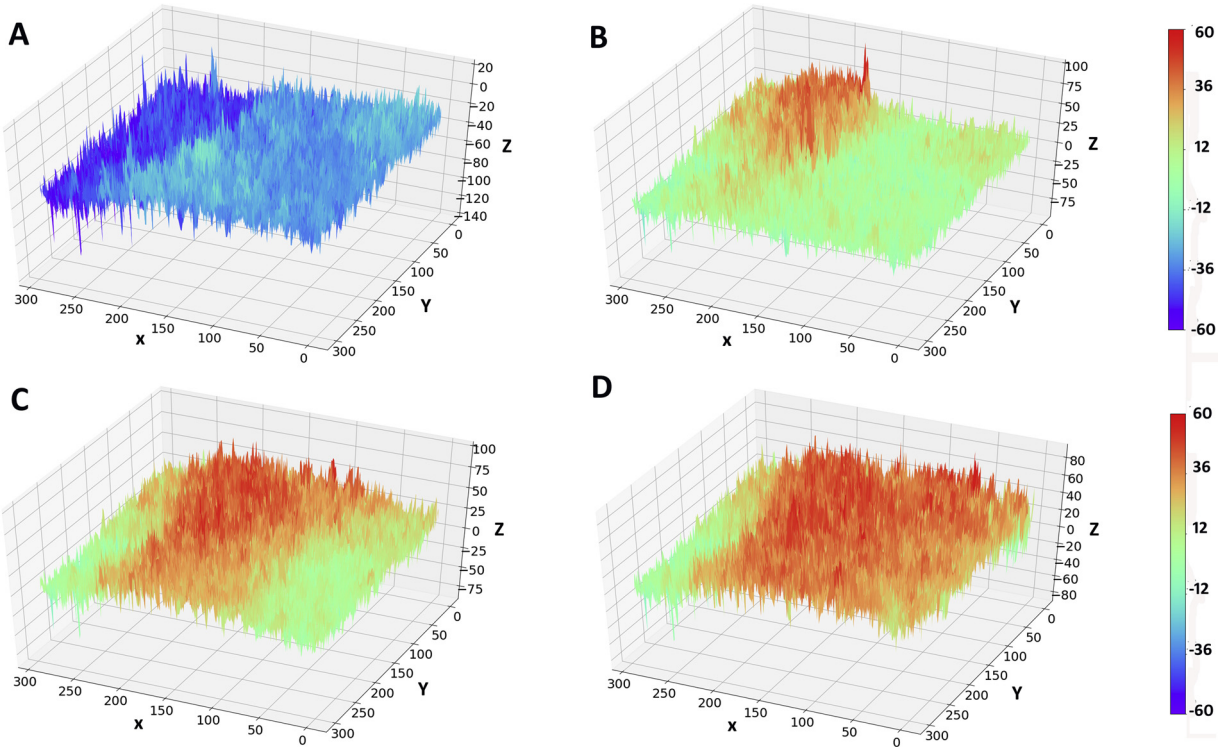

Fig. 7. 3D contour map. Bar indicates the net height.
A: 10 min, B: 30 min, C: 50 min and D: 90 min after histamine (160 mg/ml) treatment.

increased followed a linear trend. However, when the histamine dose increased to 160 mg/ml, the thickness quickly increased by 32.27% from 30 min to 50 min before reaching a plateau at 60 min, indicating that histamine-induced swelling is dose and time dependent (see Fig. 5).

Others suggest that the various layers of the mouse ear skin (e.g. epidermis, dermis and cartilage) can be identifiable on high resolution OCT [12,20,23]. However, as shown in the grayscale distribution curve (see Fig. 4), these layers were not clearly identifiable due to the limited resolution of the OCT system used in this study. So instead of directly measuring the edema zone in each layer, the full thickness of the ear was measured and the tissue swelling induced by histamine was quantified by the average full thickness changes. In addition, the edema volumes were determined.

Based on the method used by Qin and Wang in a burn model [10], similar approach was used to determine the edema volume. However, due to limited scanning capacity, this study could only extracted the edema volume from part of the histamine treated area. Nevertheless, the findings were consistence with thickness measurement, i.e. the trend in thickness change was similar to that in volume change derived from counting the voxel numbers (Fig. 5B vs Fig. 6C). The reconstructed 3D image also indicated that edema mainly developed between the dermis and cartilage on the histamine-applied side (see Fig. 6B). Nevertheless, compared to OCT measurement the manual measurement by the gauge might overestimate the thickness due to possible human error in operating the gauge (see Table 1).

The homogeneity analysis showed that, for the first time, at the higher histamine dose (160 mg/ml) the edema started from one corner of FOV (300 × 300 × 600 pixels in the Z direction) near the skin surface and slowly spreading to the entire FOV in a directional fashion. The overall homogeneity in the edema zone, however, seemed relatively high when swelling reached a plateau (see Fig. 7).

Edema is the hallmark of hyperpermeability of microvasculature. The microvascular permeability is determined by two major factors: blood flow and endothelial barrier function. Optical imaging of microvasculature presents a particular interest in physiological

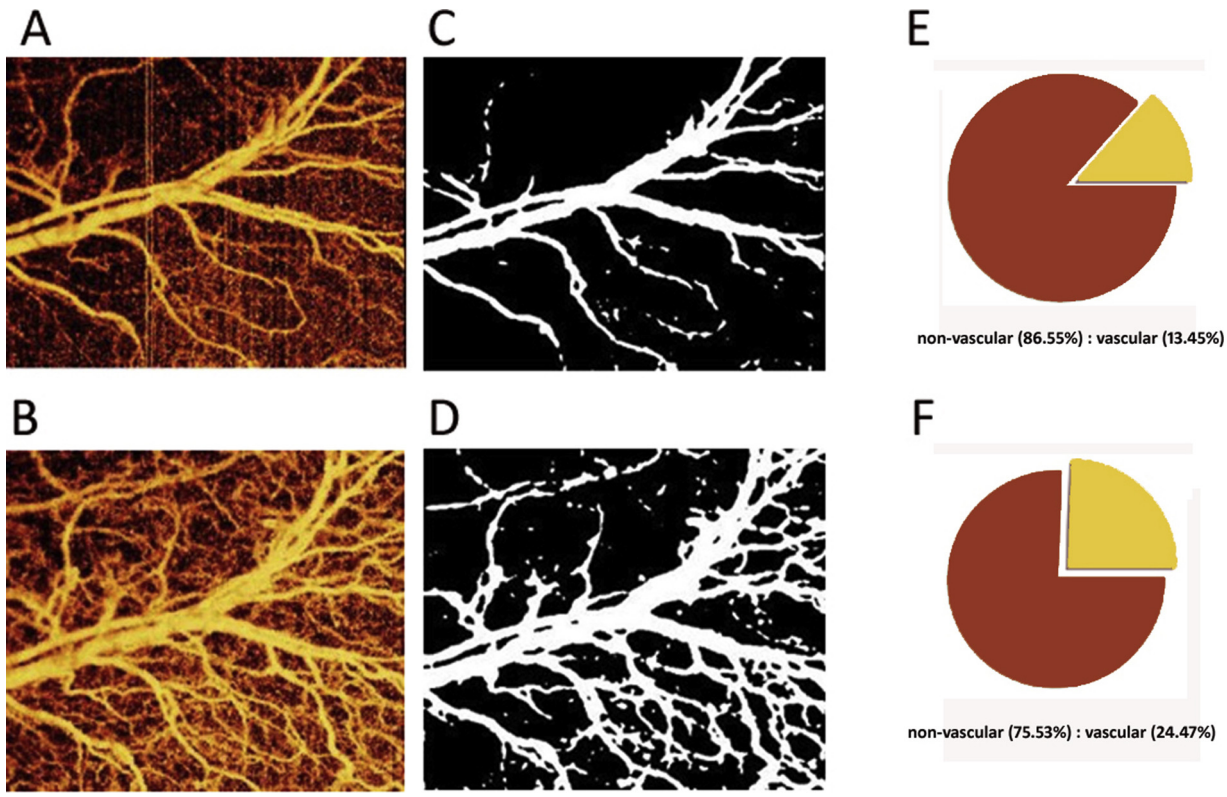

Fig. 8. Effect of histamine on microvessels.
Top panel – before histamine challenge; bottom panel – after histamine challenge. (A)-(B): Microvascular network images; (C)-(D): Binary images; (E)-(F) Proportion of microvessels in the scanned area.

measurement as well as a great challenge as due to the spatially inhomogeneous of the vessel structure and high variability in perfusion over time [24]. One of the recent advance in OCT is the use of speckle variance and phase variance techniques to visualize microvessels [25]. By analyzing both the intensity and the phase information embedded in the OCT spectral interferograms, Wang et al. were able to image the complete microvasculature network down to the capillary level [26,27]. By combining both shape-based (Hessian vesselness) and intensity-based segmentation techniques with a high speed spectral domain OCT (47,000 lines per second), the fine microvasculature networks of entire mouse ear could be reconstructed [28,29]. Liew et al. demonstrated that microvasculature in cutaneous burn scars could be extracted from polarization-sensitive OCT speckle decorrelation data [30]. Our current study used the similar technique to visualize the changes in vessel networks down to the capillary level before and after the histamine challenge in the mouse ear model (see Fig. 8). Over 10% increase in blood perfusion under 160 mg/ml for 20 min. This indicated a quick vascular response through microvessel opening and vessel dilation (vasodilation). These changes could lead to edema and ultimately the thickening of the ear.

Vasodilation can cause the increase of interstitial water content, ultimately leading to tissue swelling. The increase of interstitial water content can weaken OCT signal due to the reduction of tissue scattering, care needs to be taken to quantify OCT signals related to the increase of water content under vasodilation [31,32]. Gurjarpadhye et al. demonstrated that OCT signal could be increased via local tissue compression in which the removal of water in the compressed region increase the refraction index [33]. Nevertheless, our data suggested that speckle decorrelation (e.g. vasodilation) was more sensitive in quantifying vascular effects than thickness measurements (e.g. edema volume) without compression. In general, care should be taken not to overly compress the swollen ear during OCT examination and only measure the outer two-thirds of the ear but skin folding located at the ear base should be avoided.

Mouse ear model is a useful platform for investigating the ear skin tissue and the corresponding vessel networks. One advantage of using such model is that various non-invasive and invasive physical interventions (e.g. typing, burn, punch) which target different layers of the ear skin can be applied to generate living skin tissues for repeatable in vivo OCT measurements of the entire ear [10,27,34]. For topical drug test, manipulations of skin barrier are needed to facilitate transdermal drug delivery, even for thin ear skin. Thus, for investigating histamine mediated reactions in skin tissues acetone is often used to remove the stratum corneum ensuring histamine reactivity. Alternatively, needle pricking can be used to puncture the stratum corneum layer for OCT imaging [35].

This study only examined monolayer vessel networks located on the upper layer of the mouse ear in en face view. It should be noted that recent studies by other groups suggested that OCT-based microangiography technique can also be used to visualize vessel networks of living human skin in 3D [29,36,37]. Another limitation of this study was that only a small part of the mouse ear was examined due to the limited scanning capacity of OCT systems used. The whole ear scan can provide a better evaluation platform that might be able to reveal the swelling boundary and total volume of swelling [10]. In future study, histological examination should be carried out to confirm the swelling dynamics observed on 2D and 3D OCT scans.

5. Conclusions

This study demonstrated that in the mouse ear model acetone-induced exfoliating and histamine-induced vascular responses could be evaluated by 2D and 3D OCT scans. The histamine-induced thickness and volume changes were dose and time dependent. For the first time, contour mapping over the time course demonstrated that the histamine-induced edema started from a single spot near the skin surface and

slowly spreading directionally. OCT scan showed that histamine could induce a quick vascular response through microvessel opening and vasodilation. High resolution and high speed OCT is a robust and accurate non-invasive imaging tool for the quantitative assessment of fast dynamic process in skin swelling.

Funding sources

This work was supported in part by the National Natural Science Foundation of China (61675044) and Special Funds of the Central Government Guiding Local Science and Technology Development (2017L3009).

Disclosures

The authors have no relevant financial interests in this article and no potential conflicts of interest to disclose.

Acknowledgement

The loan of the SD-OCT by Shenzhen Certainn Technology Co., Ltd. (Shenzhen China) is appreciated.

References

[1] M. Sugaya, Y. Kuwano, H. Suga, et al., Lymphatic dysfunction impairs antigen-specific immunization, but augments tissue swelling following contact with allergens, J. Invest. Dermatol. 132 (3) (2012) 667–676.
[2] C.P. Sambuco, P.D. Forbes, Quantitative assessment of phototoxicity in the skin of hairless mice, Food Chem. Toxicol. 22 (3) (1984) 233–236.
[3] S.C. Gad, The mouse ear swelling test (MEST) in the 1990s, Toxicology 93 (1) (1994) 33–46.
[4] P. Ulrich, J. Streich, W. Suter, Intralaboratory validation of alternative endpoints in the murine local lymph node assay for the identification of contact allergic potential: primary ear skin irritation and ear-draining lymph node hyperplasia induced by topical chemicals, Arch. Toxicol. 74 (12) (2001) 733–744.
[5] V.I. Tkalcevic, B. Hrvacic, M. Bosnar, et al., Cantharidin-induced inflammation in mouse ear model for translational research of novel anti-inflammatories, Transl. Res. J. Lab. Clin. Med. 160 (2) (2012) 137–145.
[6] G. Baida, P. Bhalla, K. Kirsanov, et al., REDD1 functions at the crossroads between the therapeutic and adverse effects of topical glucocorticoids, EMBO Mol. Med. 7 (1) (2014) 42–58.
[7] J.M. Schmitt, M.J. Yadlowsky, R.F. Bonner, Subsurface imaging of living skin with optical coherence microscopy, Dermatology 191 (2) (1995) 93–98.
[8] T. Gambichler, A. Pljakic, L. Schmitz, Recent advances in clinical application of optical coherence tomography of human skin, Clin. Cosmet. Investig. Dermatol. 8 (2015) 345–354.
[9] K.B.E. Friis, L. Themstrup, G.B.E. Jemec, Optical coherence tomography in the diagnosis of actinic keratosis—a systematic review, Photodiagnosis Photodyn. Ther. 18 (2017) 98–104.
[10] W. Qin, R.K. Wang, Assessment of edema volume in skin upon injury in a mouse ear model with optical coherence tomography, Lasers Med. Sci. 31 (7) (2016) 1351–1361.
[11] K.G. Phillips, Y. Wang, D. Levitz, et al., Dermal reflectivity determined by optical coherence tomography is an indicator of epidermal hyperplasia and dermal edema within inflamed skin, J. Biomed. Opt. 16 (4) (2011) 04050301–04050303.
[12] R. Silver, A. Helms, W. Fu, et al., Using optical coherence tomography for the longitudinal non-invasive evaluation of epidermal thickness in a murine model of chronic skin inflammation, Sci. Res. Technol. 18 (2) (2012) 225–231.
[13] L. Olsen, N. Themstrup, M. De Carvalho, et al., Diagnostic accuracy of optical coherence tomography in actinic keratosis and basal cell carcinoma, Photodiagnosis Photodyn Ther. 16 (2016) 44–49.
[14] L. Themstrup, C.A. Banzhaf, M. Mogensen, et al., Optical coherence tomography imaging of non-melanoma skin cancer undergoing photodynamic therapy reveals subclinical residual lesions, Photodiagnosis Photodyn. Ther. 11 (1) (2014) 7–12.
[15] K. Ashina, Y. Tsubosaka, T. Nakamura, et al., Histamine induces vascular hyperpermeability by increasing blood flow and endothelial barrier disruption in vivo, PLoS One 10 (7) (2015) e0132367–e0132383.
[16] M. Shtessel, J. Tversky, Reliability of allergy skin testing, Ann. Allergy Asthma Immunol. 120 (1) (2018) 80–83.
[17] J. Welzel, C. Reinhardt, E. Lankenau, et al., Changes in function and morphology of normal human skin: evaluation using optical coherence tomography, Br. J. Dermatol. 150 (2) (2015) 220–225.
[18] J. Qin, J. Jiang, L. An, et al., In vivo volumetric imaging of microcirculation within human skin under psoriatic conditions using optical microangiography, Lasers Surg. Med. 43 (2) (2015) 122–129.
[19] J. Enfield, E. Jonathan, M. Leahy, In vivo imaging of the microcirculation of the volar forearm using correlation mapping optical coherence tomography (cmOCT), Biomed. Opt. Express 2 (5) (2011) 1184–1193.
[20] J. Welzel, E. Lankenau, R. Birngruber, et al., Optical coherence tomography of the human skin, J. Am. Acad. Dermatol. 37 (6) (1997) 958–963.
[21] M.S. Mahmud, D.W. Cadotte, B. Vuong, et al., Review of speckle and phase variance optical coherence tomography to visualize microvascular networks, J. Biomed. Opt. 18 (5) (2013) 050901–050913.
[22] A. Alex, B. Povazay, B. Hofer, et al., Multispectral in vivo three-dimensional optical coherence tomography of human skin, J. Biomed. Opt. 15 (2) (2010) 1–15.
[23] T. Gambichler, G. Moussa, M. Sand, et al., Applications of optical coherence tomography in dermatology, J. Dermatol. Sci. 40 (2) (2005) 85–94.
[24] J. Allen, K. Howell, Microvascular imaging: techniques and opportunities for clinical physiological measurements, Physiol. Meas. 35 (7) (2014) R91–R141.
[25] G. Chan, C. Balaratnasingam, J. Xu, et al., In vivo optical imaging of human retinal capillary networks using speckle variance optical coherence tomography with quantitative clinico-histological correlation, Microvasc. Res. 100 (2015) 32–39.
[26] R.K. Wang, S.L. Jacques, Z. Ma, et al., Three dimensional optical angiography, Opt. Express 15 (7) (2007) 4083–4097.
[27] L. An, J. Qin, R.K. Wang, Ultrahigh sensitive optical microangiography for in vivo imaging of microcirculations within human skin tissue beds, Opt. Express 18 (8) (2010) 8220–8228.
[28] S. Yousefi, R.K. Wang, Simultaneous estimation of bidirectional particle flow and relative flux using MUSIC-OCT: phantom studies, Phys. Med. Biol. 59 (22) (2014) 6693–6708.
[29] S. Yousefi, T. Liu, R.K. Wang, Segmentation and quantification of blood vessels for OCT-based micro-angiograms using hybrid shape/intensity compounding, Microvasc. Res. 97 (2015) 37–46.
[30] Y.M. Liew, R.A. Mclaughlin, P. Gong, et al., In vivo assessment of human burn scars through automated quantification of vascularity using optical coherence tomography, J. Biomed. Opt. 18 (6) (2013) 0612131–0612139.
[31] E. Sattler, R. Kaestle, G. Rothmund, et al., Confocal laser scanning microscopy, optical coherence tomography and transonychial water loss for in vivo investigation of nails, Br. J. Dermatol. 166 (4) (2011) 740–746.
[32] V.M. Kodach, J. Kalkman, D.J. Faber, et al., Quantitative comparison of the OCT imaging depth at 1300 nm and 1600 nm, Biomed. Opt. Express 1 (1) (2010) 176–185.
[33] A.A. Gurjarpadhye, W.C. Vogt, L. Yajing, et al., Effect of localized mechanical indentation on skin water content evaluated using OCT, Int. J. Biomed. Imaging 2011 (2011) 1–8.
[34] J. Yeongri, D. Suzan, Z. Zhongwei, et al., Tracking dynamic microvascular changes during healing after complete biopsy punch on the mouse Pinna using optical microangiography, PLoS One 8 (2) (2013) e57976–e57985.
[35] B. Kim, S.H. Lee, C.J. Yoon, et al., In vivo visualization of skin inflammation by optical coherence tomography and two-photon microscopy, Biomed. Opt. Express 6 (7) (2015) 2512–2521.
[36] C. Wahrlich, S.A. Alawi, S. Batz, et al., Assessment of a scoring system for basal cell carcinoma with multi-beam optical coherence tomography, J. Eur. Acad. Dermatol. Venereol. 29 (8) (2015) 1562–1569.
[37] L. Themstrup, S. Ciardo, M. Manfredi, et al., In vivo, micro-morphological vascular changes induced by topical brimonidine studied by dynamic optical coherence tomography, J. Eur. Acad. Dermatol. Venereol. 30 (6) (2016) 974–979.